# Space-Frequency Orthonormal Compensation Method for GNSS Compact Antenna Array Designs

Ezequiel A. Marranghelli
*Facultad de Ingeniería, UNLP*
*UIDET SENyT*
La Plata, Argentina
ezequiel.marranghelli@ing.unlp.edu.ar

Ramón López La Valle
*Facultad de Ingeniería, UNLP*
*UIDET SENyT*
La Plata, Argentina
lopezlavalle@ing.unlp.edu.ar

Pedro A. Roncagliolo
*Facultad de Ingeniería, UNLP*
*UIDET SENyT*
La Plata, Argentina
agustinr@ing.unlp.edu.ar

***Abstract*—In the global navigation satellites systems, the traveling time determination of the travelling signals is the main task of the receivers. For precise positioning applications, the accuracy is expected to be less than 1 ns to limit the error to the centimeters level. Hence, the influence of the responses of the antennas cannot be ignored since they can introduce delays of the order of 10 ns, which translates into errors of a few meters. The problem becomes even more complex when compact antenna arrays are used since the mutual coupling between their elements is considerable. In this work, a signal pre-processing scheme for coupled antenna arrays to compensate their space-frequency responses is described and analyzed.**

***Keywords*—Smart Antennas, Compact Arrays, Global Compensation, Orthonormal Matrix, GNSS**

## I. Introduction

The essential information that the Global Navigation Satellite Systems (GNSS) receivers must determine is the travelling time of the signals from the satellites to a reference point located in the immediate vicinity of the antenna or antenna array. This information together with the positions of the satellites are necessary to obtain the position, velocity and time (PVT) of the receiver [1]. The main benefit of using an antenna array (AA) in a GNSS receiver are the possibility of applying beamforming to increase the signal to noise ratio, reject interference or mitigate multipath [2]. Although its use implies an associated complexity in the design of the receiver, it is currently considered in critical and precise applications to ensure the integrity of the signals [3], [4]. However, in many cases there are strict space limitations which restrict the AA to be composed of a reduced number of antennas and to be extremely compact, i.e., a small array of coupled antennas. The appropriate design of a compact AA for simple array signal processing while maintaining the induced biases on the determination of the receiver's PVT to the minimum require special attention.

The incoming GNSS signals from the satellites are captured by the antenna/s, set up by the radio frequency (RF) front-ends and then digitized to subsequently go through certain stages of digital processing. In this process, the signals are modified by the equivalent frequency response of the analog and digital stages of the receiver [5]. In fact, the receiver must be able to correct or avoid these distortions. Otherwise, biases are generated in the estimates of *group and phase delays* of the GNSS signals, which is equivalent to errors in the determination of the travel time or pseudo-range [6], [7].

In a compact AA, the frequency response is not only a function of the direction of arrival (DOA), but it is also different for each antenna. The received signals will be distorted according to these functions. When considering the combination of the received signals, the distortion can be interpreted as caused by an equivalent antenna response, which also changes according to the particular combination. The conclusion is that the introduced biases of this stage are variable according the DOA. In practice, the objective is to know the induced biases at the specific DOA's of the incoming GNSS signals. When performing beamforming (BF) the weight coefficients are predefined and constant for each DOA, hence it is possible to provide the receiver of predefined tables that allows it to remove the biases. [6], [8]–[10]. However, with the presence of interferences the nullforming (NF) algorithms produce an equivalent frequency response that is highly variable according the particular scenario. Hence, the biases are no longer so simple to correct, and even less if not only spatial processing (SP) techniques are applied, but also space-time processing (STP) [11]. In [12], an analysis about the induced biases by an AA controlled by SP techniques has been done. The results suggest that, despite the differences that depends on the particular SP method, the main problem comes from the transfer function of the antennas itself. With STP techniques, the conclusions are similar [11]. Although there are solutions based on adaptive methods with minimum distortion restrictions, they require full knowledge of the responses of the antennas in the bandwidth of interest, which requires a high processing capacity and a high level of calibration precision [13]. Equalization filters can also be used to correct the effects of SP/STP [14], but the need to update the filter coefficients for each particular scenario leads to similar implementation problems.

In order to simplify these problems of the signal processing of compact AA's, it is convenient to consider a compensation technique that should preferably be global, i.e., for all the main lobe patterns region. In [15] it has been proposed a SP compensation method for compact antenna arrays with the

This work was supported by the National University of La Plata under Grant I-259 and partially by Agencia Nacional de Promoción de la Investigación, el Desarrollo Tecnológico y la Innovación, Grant PICT2017-0857.

978-1-6654-8014-7/22/$31.00 ©2022 IEEE

peculiarity of performing a linear transformation by means of an orthonormal matrix, which does not distort the radiation characteristics of the array. Additionally, it retains unaltered the statistical properties of the received signals. The purpose of this compensation is to allow that the received signals can be interpreted as those corresponding to an ideal phased array. In this paper, the proposal is extended to an STP scheme that simultaneously perform the spatial compensation and the frequency equalization of the antennas using an orthonormal/unitary matrix to obtain a virtual array that allows a wideband phased array model. This simplifies the array signal processing in the spatial domain, and reduces the induced pseudo-range biases of the acquired GNSS signals.

The rest of this work is organized as follows. Section II presents a description about the signal distortions caused by the frequency response of a multi-antenna receiver. Focusing on the most relevant factors in GNSS, the delay biases induced by an actual AA are quantified and analyzed. In Section III, a new space-frequency compensation method based on a unitary matrix is presented. Its validation is done with the previously mentioned AA. In Section V, the final conclusions are stated.

## II. Influence of the Receiver on the Pseudo-Range Determination

Figure 1 shows a block diagram of a generic GNSS receiver with a compensation stage. The $n$-th antenna response is a function defined by its radiation characteristics $g_n(f,\theta,\phi)$ and the phase differences according to its relative location $s_n(f,\theta,\phi)$, both frequency $f$ and DOA $(\theta,\phi)$ dependent. To ease notation, it is defined $s_n g_n(f,\theta,\phi) = s_n(f,\theta,\phi) g_n(f,\theta,\phi)$. The RF front-ends and the ADC's, whose frequency response vector is modelled as $\mathbf{f}(f) = [\mathrm{f}_1(f), ..., \mathrm{f}_N(f)]^T$, can also be included. Hence, the vector that store the complete response is $\mathbf{h}$ and can be defined as follows,

$$\mathbf{h}(f,\theta,\phi) = \mathbf{sg}(f,\theta,\phi) \circ \mathbf{f}(f). \tag{1}$$

where the operator $\circ$ is the Hadamard product.

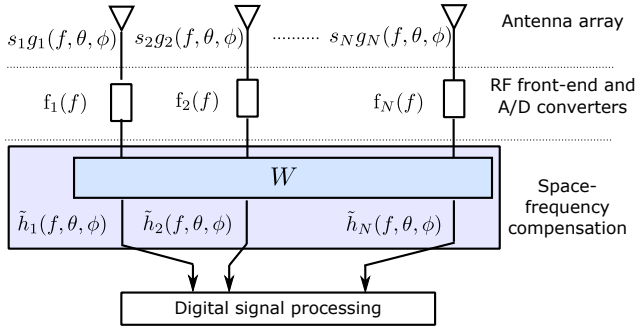


Fig. 1. Model of a GNSS receiver with a space-frequency digital compensation stage.

The GNSS signals transmitted by the satellites impinge on the antennas of the receiver after an elapsed time $\tau_0$. These signals become distorted by the responses of each RF channel $h_n(f,\theta,\phi)$, or the equivalent response $h_{BF/NF}(f,\theta,\phi)$ which is a result of applying BF/NF. Consequently, the receiver obtains a distorted replica of the signal which typically presents an additional time delay. A graphical representation is illustrated in Fig. 2, where the A/D conversion, the additive noise and other distortion effects over the signals have been omitted for the sake of simplicity. Therefore, the important characteristics that we need to rescue for the PVT determination are the group delay $\delta\tau_0$ and phase delay $\delta\phi_0$ biases that are introduced by the antenna array and subsequent stages. In terms of the navigation solutions, the group delay bias can produce position errors of $c \cdot \delta\tau_0$ meters level, being $c \cong 3 \cdot 10^8$ m/s the speed of light in vacuum. The phase delay bias has influence in more precise measurements given that its effect is of the order of centimeters.

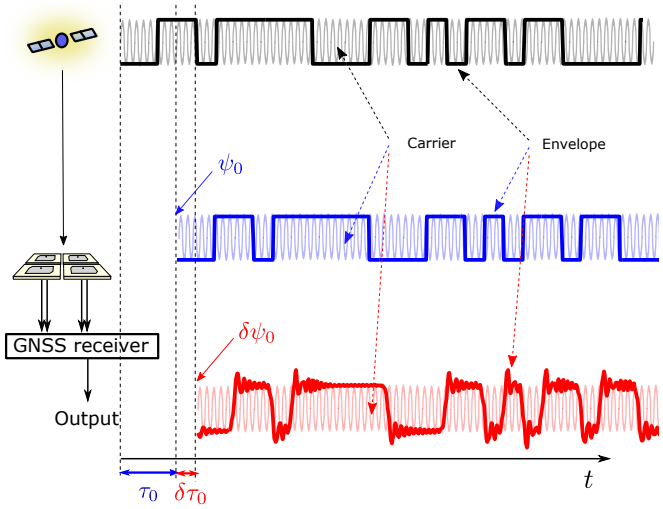


Fig. 2. Group delay and phase delay in a received GNSS signal.

Hereafter, it is assumed that the receiver and the satellites are perfectly synchronized in time and that the wireless channel is ideal, that means that all other possible influence factors over the pseudo-range are omitted. Hence, it is only considered the traveling time of the desired signal together with the biases incorporated by the receiver. Given a GNSS satellite signal expressed in baseband, $d(t)$, when it arrives to the reference point of the receiver it becomes $A_0 d(t-\tau_0)e^{j\phi_0}$, where $A_0$ in the signal amplitude, $\phi_0$ is its phase referred to the carrier frequency (particularly $f_c = 1575.42$ MHz for the L1 band of GPS), and $\tau_0$ is the traveling time of the signal. If it is also considered the existence of $J$ interference signals, $I_j(t)$, it can be expressed as,

$$y(t) = A_0 d(t-\tau_0)e^{j\phi_0} + \sum_{j=1}^{J} I_j(t)\,, \tag{2}$$

Its autocorrelation function (averaged in time, for cyclically stationary power signals) is obtained as follows:

$$R_{yy}(\tau) = \langle \mathrm{E}\{y(t)y^*(t-\tau)\}\rangle$$

$$R_{yy}(\tau) = \lim_{T\to\infty} \frac{1}{T} \int_{-T/2}^{T/2} \mathrm{E}\{y(t)y^*(t-\tau)\}dt \qquad (3)$$

where $\mathrm{E}\{\cdot\}$ denotes the mathematical expectation, in order to include random signals in the model. Doing the calculations and using similar definitions for the autocorrelations of the GNSS signals, $R_{dd}(\tau)$ and the interferences, $R_{I_jI_j}(\tau)$, one obtains,

$$R_{yy}(\tau) = A_0^2 R_{dd}(\tau) + \sum_{j=1}^{J} R_{I_jI_j}(\tau)\,, \qquad (4)$$

where the equality is fulfilled when the signal and each one of the interferences are completely uncorrelated to each other. According to the theorem of Wiener-Khintchine [16], applying the Fourier transform we obtain the Power Spectral Density (DEP):

$$S_{yy}(f) = A_0^2 S_{dd}(f) + \sum_{j=1}^{J} S_{I_jI_j}(f)\,, \qquad (5)$$

being $S_{dd}$ the DEP of the baseband signal, and $S_{I_jI_j}$ the DEP of the $j$-th interference.

Therefore, the vector of received signals, $\mathbf{x}(t)$, consists of the $y(t)$ signal affected by the transfer functions of each of the channels of the receiver. Besides, it includes the antenna array noise vector, $\mathbf{e}(t)$, which is also weighted by the transfer functions of the RF front-end. It is assumed to be white noise with DEP $\mathrm{N}_0/2$. Then, the DEP of $\mathbf{x}(t)$ is [17], [18],

$$S_{\mathbf{xx}}(f) = A_0^2 S_{dd}(f)|\mathbf{h}(f,\theta_0,\phi_0)|^2 + \cdots \\ \cdots + \sum_{j=1}^{J} S_{I_jI_j}(f)|\mathbf{h}(f,\theta_j,\phi_j)|^2 + \frac{\mathrm{N}_0}{2}|\mathbf{f}(f)|^2\,. \qquad (6)$$

Hence, the corresponding autocorrelation function of $\mathbf{x}(t)$ is,

$$R_{\mathbf{xx}}(\tau) = \int_{-\infty}^{\infty} S_{\mathbf{xx}}(f) e^{j2\pi f\tau} df\,. \qquad (7)$$

Correspondingly, the intercorrelation function between the signals vector and the local reference signal $d(t)$ can be expressed as

$$R_{\mathbf{x}d}(\tau) = \langle \mathrm{E}\{\mathbf{x}(t)d^*(t-\tau)\}\rangle\,. \qquad (8)$$

If we consider a single antenna that presents an ideally isotropic response $h(f,\theta_0,\phi_0) = 1$ for the bandwidth of design, then the intercorrelation results,

$$R_{xd}^{h=1}(\tau) = A_0 e^{j\phi_0} R_{dd}(\tau-\tau_0) + \sum_{j=1}^{J} R_{I_jd}(\tau) + R_{ed}(\tau)\,, \qquad (9)$$

where it is expected that the two latest terms be approximately null given that it is assumed that the signal is completely uncorrelated to the interferences $R_{I_jd}(\tau) = 0$ and the noise $R_{ed}(\tau) = 0$. Hence, $R_{xd}^{h=1}(\tau)$ is maximum when $\tau = \arg_\tau \max\{|R_{xd}^{h=1}(\tau)|\} = \tau_0$, and in such a case the phase of the intercorrelation coincides with $\phi_0$. Then, with this ideal antenna, $h = 1$, the search for the maximum of $R_{xd}^{h=1}(\tau)$ would allow to obtain unbiased estimates of $\tau_0$ y $\phi_0$. In the frequency domain, the same information can be expressed by means of the power interdensity:

$$R_{xd}^{h=1}(\tau) \quad \overset{F}{\supset} \quad S_{xd}^{h=1}(f) = A_0 e^{j\phi_0} S_{dd}(f)\, e^{-j2\pi f\tau_0}\,, \qquad (10)$$

For an ideal antenna whose phase center does not match with the chosen reference point, its response can be written as $h = s = e^{j2\pi f \mathbf{o}_0^T\mathbf{p}/c}$, being $\mathbf{p}$ the position vector of the antenna, and $\mathbf{o}_0$ the directional cosines in the DOA of observation $(\theta_0,\phi_0)$. The power spectral interdensity results,

$$S_{xd}^{h=s}(f) = A_0 e^{j\phi_0} S_{dd}(f)\, e^{j2\pi f(-\tau_0+\mathbf{o}_0^T\mathbf{p}/c)}\,, \qquad (11)$$

and the corresponding intercorrelation function is,

$$R_{xd}^{h=s}(\tau) = A_0 \int_{-\infty}^{\infty} S_{dd}(f)\, e^{j\phi_0 + j2\pi f(\tau-\tau_0+\mathbf{o}_0^T\mathbf{P}/c)} df\,,$$

$$R_{xd}^{h=s}(\tau) = A_0 e^{j\phi_0} R_{dd}(\tau-\dot{\tau}_0)\,, \qquad (12)$$

being $\dot{\tau}_0 = \tau_0 - \mathbf{o}_0^T\mathbf{P}/c$, while the phase delay $\phi_0$ is not modified.

If we finally consider an antenna (and its RF front-end) whose response behaves as $h(f,\theta_0,\phi_0) = \mathrm{g}(f,\theta_0,\phi_0)\mathrm{f}(f)e^{j2\pi f\mathbf{o}_0^T\mathbf{P}/c}$, the power interdensity experiences changes both in module and phase, and as a consequence, the intercorrelation is also affected with changes. Mathematically can be expressed as,

$$R_{xd}^{h}(\tau) = A_0 \int_{-\infty}^{\infty} S_{dd}(f)|h(f,\theta_0,\phi_0)|^2 \cdots \\ \cdots\ e^{j\phi_0 + j2\pi f(\tau-\tau_0) + j\angle h(f,\theta_0,\phi_0)} df\,. \qquad (13)$$

The influence of the antenna response is evident, and its effects are represented qualitatively in Fig. 2. Now taking into consideration an AA, when performing BF/NF with SP techniques we obtain an equivalent response

$$h_{BF/NF} = \sum_{n=1}^{N} c_n h_n(f,\theta_0,\phi_0). \qquad (14)$$

In this case, the intercorrelation is variable as a function of the particular weight vector $\mathbf{c}$ that is used, and it must be considered that it modifies the induced biases for both the ideal and non-ideal antenna responses.

From a quantitative point of view, it must be determined which is the effect of the antennas or the AA in terms of the resulting group delay $\dot{\tau}_0 = \tau_0 + \delta\tau_0$ and carrier phase delay $\dot{\phi}_0 = \phi_0 + \delta\phi_0$, being $\delta\tau_0$ and $\delta\phi_0$ the receiver induced biases. Since an analytical deduction is not immediate, in the following subsection a numerical approximation based on least squares estimation is chosen.

### A. Group and phase delays estimation

Typically, the antennas are designed so that the transfer function or frequency response has practically constant amplitude in the bandwidth of interest and its phase remains linear, which is an appropriate approximation for narrowband antennas. With this assumption, the phase presents a dependency that is expressed as $\sim j(\delta\phi_0 + 2\pi f \delta\tau_0)$, being $\delta\phi_0$ and $\delta\tau_0$ the denominated phase and group delay biases. However, these parameters are not constant given that the transfer function of an antenna is DOA dependent, and a coupled AA has a different function to each one of them. Hence, to perform precise positioning in GNSS it is required to know and remove their effects.

In [17] a simple approximation based on least squares is defined, which can be used to estimate the biases introduced by an actual antenna or AA. The formulation consist of defining the phase of the transfer function that has been presented in (13) as $\alpha(f, \theta_0, \phi_0)$, and to find the polynomial of degree 1 that best fits it in terms of a weighted linear regression. The weighting factor takes into account that the DEP of the signal, $S_{dd}(f)$, has the influence of the frequency response of the antenna/s and RF front-end/s, as it is shown in (13). In summary, the fit is performed considering $\alpha(f, \theta_0, \phi_0) \approx \alpha_0 + \alpha_1 f$, where the parameters approximate the carrier phase $\dot{\psi}_0 \cong \alpha_0$, and code delay $\dot{\tau}_0 \cong -\alpha_1/2\pi$, in order to discriminate the biases $\delta\psi_0$ and $\delta\tau_0$.

In this work, we adopt the antenna array proposed in [19] as case of study. This array has a considerably coupling level which is beneficial by design.

### B. Characterization of the AA under test

The AA consists of four microstrip antennas over the same Ro4350B substrate PCB and sharing the same ground plane. Each antenna has a single coaxial feed port, and their separation distance is $d = \lambda/3$, being $\lambda$ the wavelength at the carrier frequency of GPS, $f_c = 1575.42\,\text{MHz}$. The AA and its dimensional parameters are shown in Fig. 3. This particular design, when used together with the proposed orthogonal transformation, can be treated as an ideal phase array for space processing purposes [19].

Figure 4 presents a map of the estimated group delay of all the antennas for each of the DOA's of the upper hemisphere, where the array radiation is higher. This group delay biases has been translated to pseudo-range biases. In general, it is verified that there is an average error of approximately $-3$ m in a large part of the space. Then, deviations around $\pm 1$ m are observed in various sectors, even reaching differences of up to $\pm 2$ m, mainly for low elevation angles. These variations show the level of uncertainty that exists between DOA's and antennas. Moreover, if BF/NF is performed the equivalent response has a new biases map that can change according the weighting coefficients needed for the combination [12]. For the following evaluations, the Orthogonal Projection Beamforming (OPB) is used either for BF/NF [20].

*1) Group delay when performing BF:* When BF is applied, an equivalent group delay pattern is obtained as a function of the particular vector of weights that has been used to direct the beam in the direction in which the signal is assumed to come from. For each combination we are interested in knowing the delay only in the DOA of the desired signal. Therefore, each DOA in the map that is presented in Fig. 5(a) shows the obtained group delay when the BF technique is applied to maximize the gain in that direction, so every DOA in the map arises from a different BF combination. It can be seen that the resulting map is quite homogeneous, with smooth variations in a relatively minor range. So the pseudo-range errors produced by the receiver when a satellite traverses across the space may vary in the range $\sim [-3.5, -2.5]$ meters at most. This means that when performing BF, the uncertainty in the group delay is significantly reduced in comparison to the differences already seen in the individual antennas because they are approximately neutralized by the averaging.

*2) Group delay when performing NF:* In the presence of interference/s, the group delay in the direction of the desired signal also depends on the location of the interference/s. Suppose a particular case in which there is an interference located at $(90°, 270°)$, and OPB is applied to mitigate it while the gain in each of the possible directions in which the desired signal arrives is maximized. The group delay map is presented in Fig. 5(b). This particular case confirms the assumptions and shows that in these situations the unwanted delay variations are considerable and approximately equal to or even greater than the individual antennas.

## III. Space-frequency compensation

In order to compensate for these effects, a joint space-frequency compensation will be developed. The proposed array [19] was designed to be used in conjunction with a unitary spatial compensation matrix. The following development consists of a new method that simultaneously compensates in space and frequency, also with a single unitary matrix. Hence, it is an extension of the previous version, and it will be analyzed on the already presented AA design.

### A. Compensation scheme

This method is intended to reduce the differences that the antennas present among their radiations patterns in space and frequency. The purpose is to obtain a virtual phased array to simplify the following signal processing stages. In Fig. 6 the structure of this digital compensation stage is shown. Each one of the samples of the received signal by the $n$-th antenna in a specific time instant, $t_i$, is $x_n[i]$. By using time delay blocks $z^{-1} = e^{-j2\pi f/f_m}$, where $f_m$ is the sampling frequency, the samples of $K$ time instants are stored. Assuming $K$ odd, for each time instant $t_i$ the data $x_n[i-k]$ is stored, with $k = -(K-1)/2, \cdots, 0, \cdots, (K-1)/2$. This definition with instants before and after the central one is convenient since it provides symmetry in the phase evolution, which allows better results to be achieved in this type of development [21]. If the different samples are grouped in the same dimension then the

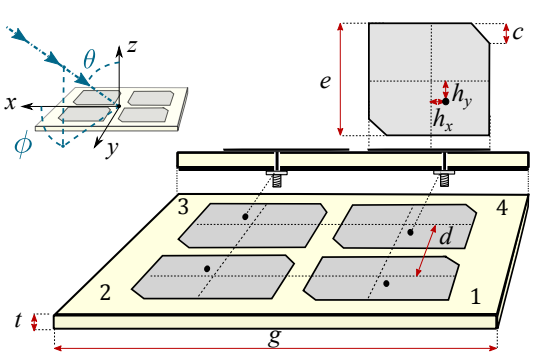


| Param. [mm] |
|---|
| $\lambda = 190.4$ |
| $g = 140$ |
| $d = 63.4$ |
| $e = 48.45$ |
| $c = 4.3$ |
| $h_x = 0.6$ |
| $h_y = 10.5$ |
| $t = 1.524$ |

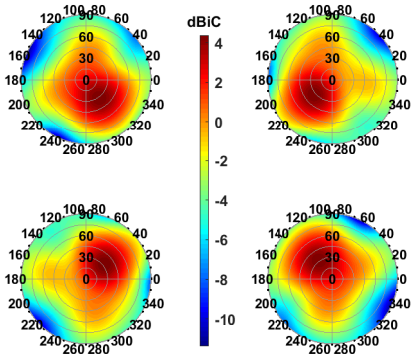


(a) AA geometry.

(b) RHCP realized gain patterns, $|\mathbf{h}(\theta, \phi)|$.

Fig. 3. Four elements planar AA and its radiation patterns (without compensation).

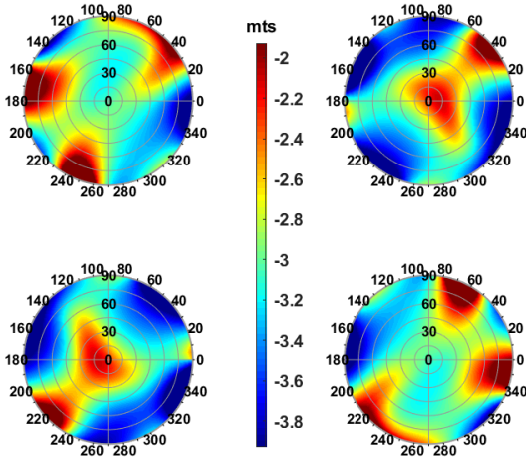


Fig. 4. Group delay patterns of the AA.

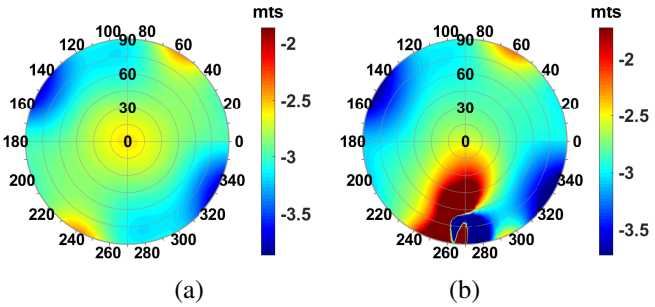


(a) (b)

Fig. 5. Resulting group delay when performing (a) BF to each DOA, (b) NF to each DOA with a null in $(90°, 270°)$.

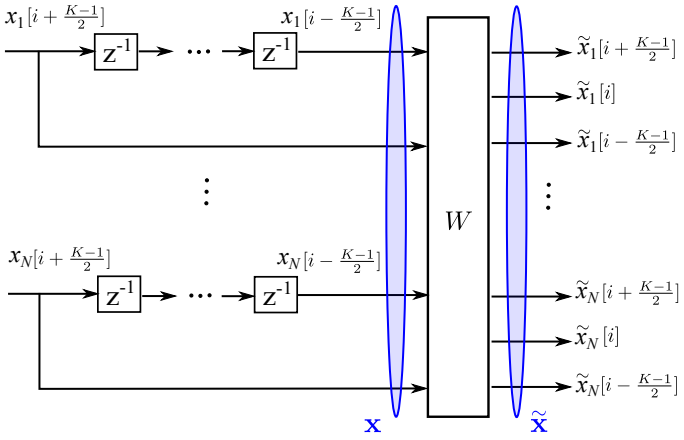


Fig. 6. Space-frequency compensation scheme.

vector $\mathbf{x}$ can be constructed, which has a total of $N \cdot K$ rows and whose elements are indicated as $x_{n,[i-k]}$. Without loss of generality, we assume $i = 0$ and that only one signal exists and comes from $(\theta_0, \phi_0)$. Hence, the spectrum of the signals is affected by, $h_n(f, \theta_0, \phi_0)\ z^{-k}$.

When applying the transformation, the vector of signals $\tilde{\mathbf{x}}$ is obtained, which has the same dimensions and therefore represents the signals of $N$ antennas and $K$ consecutive instants of time, now dependent on the responses of the compensated virtual array, $\tilde{h}_n(f, \theta_0, \phi_0)\ z^{-k}$. It can be noted that the term $z^{-k}$ already has a linear dependence on frequency, therefore it is not necessary to incorporate it in the process of searching for the objective array response $\mathring{\mathbf{h}}$. The compensation will be performed for the discrete set of DOA's, $(\theta_p, \phi_p)$ with $p = 1, \cdots, P$, that cover the radiation hemisphere of the antennas, and for a certain set of frequencies, $f_l$ with $l = 1, \cdots, L$, that are representative of the signal and antennas' bandwidth. Therefore, the designed array matrix $H$ and the target array matrix $\mathring{H}$ must be defined, where each of them have dimensions $N \times (P \cdot L)$.

The proposal to find the appropriate features for the target array and the corresponding unitary transformation matrix is similar to the development presented in [19]. The steps to effectuate are the same, starting with the initial objective matrix $\mathring{H}_A$, going on to obtain the optimized response $\mathring{H}_B$, and finally the objective array response $\mathring{H}$.

*1) Initial objective array response, $\mathring{H}_A$:* The magnitude and phase of the initial response are defined as,

$$|\mathring{h}^A_{n,pl}| = \sqrt{\frac{1}{N}\sum_{m=1}^{N} |h_{m,pl}|^2}\,, \tag{15}$$

$$\angle \mathring{h}^A_{n,pl} = \frac{2\pi f_l d_n}{c} \sin(\theta_p) \cos\left(\phi_p - \varphi_n\right), \tag{16}$$

where $d_n = d/\sqrt{2} = c/(3\sqrt{2}f_c)$ y $\varphi_n = \varphi_{ref} - 2\pi\frac{(n-1)}{N}$ are the polar coordinates of each antenna relative to the geometric center of the array, $\varphi_{ref} = 3\pi/4$ is the reference angle that coincides with the orientation of the antenna labeled 1, $f_c$ is the center frequency of design, and $pl = p + (l-1)\cdot P$ is the index that combines $p$ and $l$ in the same matrix dimension.

*2) Optimized objective array response, $\mathring{H}_B$:* The iterative process is based on the steepest descent method, which tries to optimize the phase of all the terms of $\mathring{H}_A$. The structure of the algorithm is:

1) Initialize $\mathring{H}_B = \mathring{H}_A$, $R = H^H H$, $\mathring{R}_B = \mathring{H}_B^H \mathring{H}_B$, $\gamma_B = \|R - \mathring{R}_B\|_F^2$, and the step size $\alpha$.
2) The gradient of $\gamma_B$ about the phase of each term of $\mathring{H}_B$ is the matrix $\delta$ that is calculated as,

$$\delta_{n,pl} = 4\,\Re\left\{\sum_{ql=1}^{P\cdot L}\left[j\mathring{h}_{n,pl}\,\mathring{h}^*_{n,ql}\,\left(\mathring{r}_{pl,ql} - r_{pl,ql}\right)\right]\right\}, \tag{17}$$

   where $r_{pl,ql}$ and $\mathring{r}_{pl,ql}$ are the elements of the matrices $R$ and $\mathring{R}_B$ respectively.
3) Update the phases in the opposite direction of the gradient wit a step $\alpha$,

$$\angle \mathring{H}_B = \angle \mathring{H}_B - \alpha\delta, \tag{18}$$

   then the correlation matrix $\mathring{R}_B$ and the cost function $\gamma_B$.
4) If an acceptable value for $\gamma_B$ has not yet been achieved, or some other break condition has not been met, check the convergence of $\gamma_B$, update $\alpha$ if necessary, and then return to the point 2.

*3) Objective array response, $\mathring{H}$:* Now for the virtual array, the steering vectors $\mathring{S}$ and the gain of the antennas $\mathring{G}$ may be derived from the previous results. The gains retain their originally defined magnitudes, but the phases arise from averaging,

$$|\mathring{g}_{n,pl}| = |\mathring{h}^B_{n,pl}|, \qquad \angle \mathring{g}_{n,pl} = \frac{1}{N}\sum_{m=1}^{N} \angle \mathring{h}^B_{m,pl}\,. \tag{19}$$

The remaining variations of the phase components of $\mathring{H}_B$ are incorporated to the matrix $\mathring{S}$ as indicated next,

$$\angle \mathring{s}_1(f_l, \theta_p, \phi_p) = \frac{1}{N}\sum_{m=1}^{N} \psi_m\big(f_l, \theta_p, \phi_p + 2\pi\frac{m-1}{N}\big)\,, \tag{20}$$

$$\angle \mathring{s}_{n+1}(f_l, \theta_p, \phi_p) = \angle \mathring{s}_n(f_l, \theta_p, \phi_p + 2\pi\frac{1}{N})\,, \tag{21}$$

where $\psi_m(f_l, \theta_p, \phi_p) = \angle \mathring{h}^B_{m,pl} - \angle \mathring{g}_{m,pl}$.

In this way it is possible to obtain the matrix of averaged responses,

$$\mathring{H} = \mathring{S} \circ \mathring{G}\,. \tag{22}$$

*4) Orthonormal transformation and virtual array:* Since we already have the structure of the matrices $H$ and $\mathring{H}$, we can now add the time delays. We define the matrices named $H^z$ and $\mathring{H}^z$, whose elements are,

$$h^z_{nk,pl} = h_n(f_l, \theta_p, \phi_p)\; e^{-j2\pi f_l k/f_c}\,, \tag{23}$$

$$\mathring{h}^z_{nk,pl} = \mathring{h}_n(f_l, \theta_p, \phi_p)\; e^{-j2\pi f_l k/f_c}\,, \tag{24}$$

being $nk = n + (k-1)\cdot N$ the combined index of $n$ and $k$. Thus, the unitary matrix $W$ is calculated as,

$$W = UV^H\,, \tag{25}$$

being $U$ and $V$ the unitary matrices of left and right eigenvectors of the Singular Value Decomposition (SVD) of the matrix $\mathring{H}^z Q Q^H H^{zH}$, where $Q$ it a diagonal matrix that allows assigning different weights to each DOA. This leads to the following approximate equality,

$$WH^z = \tilde{H}^z \approx \mathring{H}^z. \tag{26}$$

Although the memory and processing capability requirements for obtaining the $W$ matrix are considerable, this process only needs to be done once. In contrast, applying this transformation on a receiver does not consume significant resources.

### *B. Validation*

Next, the space-frequency compensation of the proposed array is performed. For the development, $P$ DOA's were considered, each $5°$ in the range $0° \leq \theta \leq 90°$ and $0° \leq \phi < 360°$. The $L$ frequencies were defined in a 10 MHz bandwidth around $f_c$, which correspond to the set $\{f_l\}_{l=1}^{11} = f_c + \{0, \pm1, \pm2, \pm3, \pm4, \pm5\}$MHz.

*1) Characterization of the compensated antennas:* Working with a single temporal sample is defined as the case $K = 1$, it is equivalent to perform an spatial compensation as done in [19], and whose results are presented in Fig. 7. By using a larger number of samples ($K > 1$) it has been verified that the quality of the compensation in the space domain is preserved as expected, and in the following its performance in the frequency domain will be analyzed.

In Fig. 8 the group delay maps for the four compensated antennas with $K = 3$ are presented. It can be seen that in addition to correcting the average delay value, in certain DOA's it was possible to reduce the existing deviations. It is at higher elevations where the greatest differences still persist. Although a gradual improvement is achieved as more $K$ time instants are processed, in the present arrangement the corrections converge quickly without presenting great differences for high $K$. Naturally, the latter occurs because a limit is reached in terms of the possibility of homogenizing the bias maps for all the selected DOA's with the same transformation.

For practical purposes, it is interesting to continue by evaluating the resulting bias after performing BF or NF.

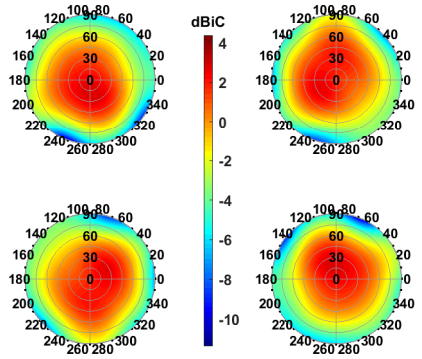


Fig. 7. Realized gain patterns with the spatial compensation (K=1).

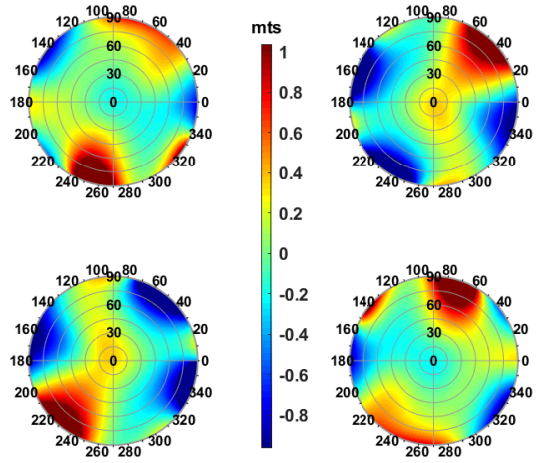


Fig. 8. Group delay patterns of the compensated AA ($K = 3$).

*2) Characterization of the group delay bias for BF:* In this comparison we analyze the resulting group delay diagram when performing BF in the direction of the desired signal, which runs through each of the possible DOA's of the upper hemisphere with a step of $5°$. Fig. 9 shows the group delay maps when performing BF with the AA for each processing scheme, that is, uncompensated (NC) and $K = 3$. Both present significant differences between them. Group delay variations have been noticeably reduced at low elevations, keeping a practically constant value as is desirable. At higher elevations the variations have not been corrected. In a certain way, this is related to the fact that the compensation aims to neutralize the differences between antennas, but it does not ensure that better results are obtained in BF.

Although the calculation of the compensation matrix $W$ takes into account the responses of the antennas, there is more influence by those DOA's where their gain is greater. By means of the weight matrix $Q$, the relative weight that each DOA acquires can be graded in a compromise relationship that allows for better compensation in certain sectors compared to others. The results presented in Fig. 9 are equivalent to using

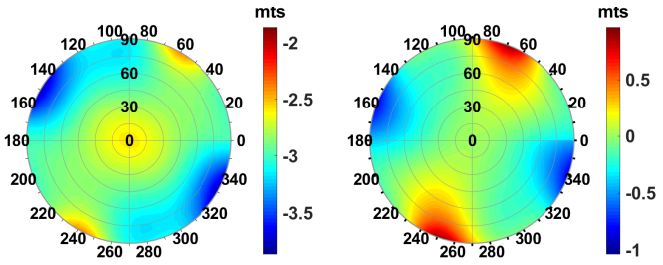


(a) NC. (b) $K = 3$.

Fig. 9. Group delay obtained when performing BF to each DOA. Comparison without and with compensation.

an identity matrix called $Q0$. Consider a weight matrix $Q1$ whose elements on the diagonal are,

$$Q1_{pl,pl} = \frac{1}{|\mathring{h}_{n,pl}|}, \tag{27}$$

with $pl = p+(k-1)\cdot P$ and $n = 1$ since all the target antennas have the same magnitude. If $Q1$ is used instead of $Q_0$, then it is possible to reduce the priority imbalance in terms of the calculation of the $W$ matrix between the different DOA's. In Fig. 10 the new delay bias graphs are presented, where it can be seen that at high elevations the delay deviations are reduced to a certain extent, while no significant changes are found for lower elevations. Therefore, the use of a weight matrix can be of help to improve the performance at high elevations in cases where it is required, for instance when the signals coming from grazing orientations are commonly recovered.

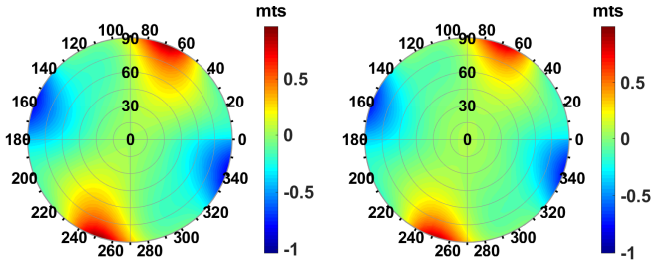


(a) $K = 3$, $Q0$. (b) $K = 3$, $Q1$.

Fig. 10. Group delay when performing BF to each DOA. Comparison regarding the use of a weight matrix.

*3) Characterization of the group delay bias for NF:* As shown above, the group delay biases are increased when performing NF. In Fig. 11 it can be seen that the array incorporates considerable variations in the map of delay biases when trying to cancel an interference located at $(90°, 270°)$ while maximizing the gain in other DOA's. As with BF, the $K = 3$ compensation manages to significantly reduce the variations for low elevations. In the region close to the interference, it is in vain to analyze the delay because the response of the array has very low gain. Observing other sectors, it can be concluded that it has not been possible to completely reduce the variations at high elevations either. But

again, it is possible to consider the use of a matrix of weights $Q1$ in order to reduce the variations at high elevations. The results of this last case are presented in Fig. 12, where a significant improvement is observed.

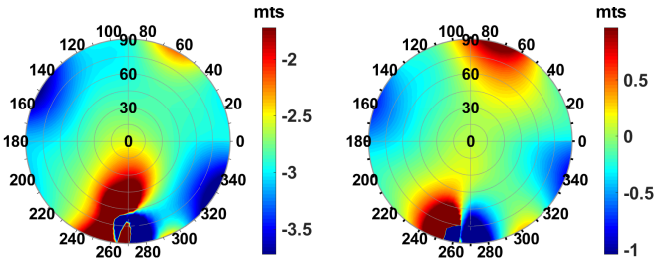


(a) NC. (b) $K = 3$.

Fig. 11. Group delay when performing NF to $(90°, 270°)$ and maximizing every other DOA. Comparison without and with compensation.

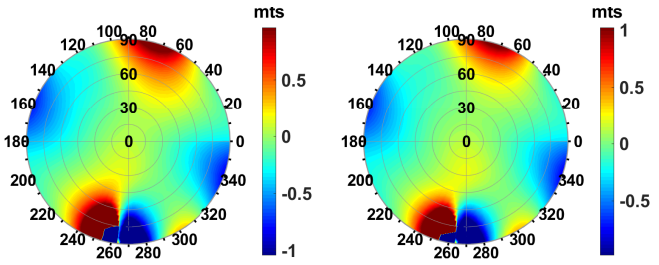


(a) $K = 3$, $Q0$. (b) $K = 3$, $Q1$.

Fig. 12. Group delay when performing NF to $(90°, 270°)$ and maximizing every other DOA. Comparison regarding the use of a weight matrix.

## IV. Conclusions

In the present work it has been verified that the level of uncertainty produced by an array of coupled antennas in the determination of the position of a GNSS receiver can be of the order of a few meters. From this point of view, the development of broadband compensation techniques is interesting because they help to avoid relying on the frequency responses of the antennas in order to remove their effects. The development presented here provides an adequate space-frequency compensation scheme for compact arrays. The results obtained show that it is possible to globally reduce the uncertainty with a single transformation matrix which is in fact unitary, thus does not alter the noise statistics between samples and between channels, neither the array radiation properties. In summary, this method allows effective signal processing while reducing induced biases on the PVT solution for GNSS applications that use small arrays. It may also be considered to be used in other applications that require simple yet effective signal processing with compact AA.

## References


[1] E. Kaplan and C. J. Hegarty, *Understanding GPS. Principles and applications*, 2nd ed. Boston - London: Artech House, 2006.

[2] F. Gross, *Smart antennas for wireless communications: with MATLAB*. McGraw-Hill, Inc, 2005.

[3] D. S. De Lorenzo, J. Rife, P. Enge, and D. M. Akos, "Navigation accuracy and interference rejection for an adaptive GPS antenna array," *Proc. Inst. Navig. - 19th Int. Tech. Meet. Satell. Div. ION GNSS 2006*, vol. 2, no. August, pp. 763–773, 2006.

[4] M. Cuntz, A. Konovaltsev, and M. Meurer, "Concepts, Development, and Validation of Multiantenna GNSS Receivers for Resilient Navigation," *Proc. IEEE*, vol. 104, no. 6, pp. 1288–1301, 2016.

[5] I. J. Gupta, I. M. Weiss, and A. W. Morrison, "Desired Features of Adaptive Antenna Arrays for GNSS Receivers," *Proc. IEEE*, vol. 104, no. 6, pp. 1195–1206, 2016.

[6] U. S. Kim, D. De Lorenzo, J. Gautier, P. Enge, J. A. Orr, D. D. Lorenzo, J. Gautier, P. Enge, and J. A. Orr, "Phase Effects Analysis of Patch Antenna CRPAs for JPALS," *17th Int. Tech. Meet. Satell. Div. Inst. Navig. ION GNSS 2004*, pp. 1531–1538, sep 2000.

[7] U. S. Kim, "Analysis of Carrier Phase and Group Delay Biases Introduced by CRPA Hardware," in *Proc. 18th Int. Tech. Meet. Satell. Div. Inst. Navig. ION GNSS 2005*, 2005, pp. 635–642.

[8] A. Konovaltsev, M. Cuntz, L. A. Greda, M. V. T. Heckler, and M. Meurer, "Antenna and RF front end calibration in a GNSS array receiver," *Proc. IEEE IMWS "RF Front. Softw. Defin. Cogn. Radio Solut.*, pp. 103–106, oct 2010.

[9] S. Backén, D. Akos, and M. Nordenvaad, "Post-processing dynamic GNSS antenna array calibration and deterministic beamforming," *ION GNSS*, 2008.

[10] S. Daneshmand, N. Sokhandan, M. Zaeri-Amirani, and G. Lachapelle, "Precise calibration of a GNSS antenna array for adaptive beamforming applications," *Sensors (Switzerland)*, vol. 14, no. 6, pp. 9669–9691, 2014.

[11] D. S. De Lorenzo, S. C. Lo, P. K. Enge, and J. Rife, "Calibrating adaptive antenna arrays for high-integrity GPS," *GPS Solut.*, vol. 16, no. 2, pp. 221–230, apr 2012.

[12] E. A. Marranghelli, G. Ramon Lopez La Valle, and P. A. Roncagliolo, "A Spatial Signal Processing Review for Practical GNSS Antenna Arrays," in *2018 IEEE Bienn. Congr. Argentina, ARGENCON 2018*, San Miguel de Tucumán, Argentina.

[13] A. J. O'Brien and I. J. Gupta, "Mitigation of adaptive antenna induced bias errors in GNSS receivers," *IEEE Trans. Aerosp. Electron. Syst.*, vol. 47, no. 1, pp. 524–538, sep 2011.

[14] R. L. Fante and J. J. Vaccaro, "Wideband cancellation of interference in a GPS receive array," *IEEE Trans. Aerosp. Electron. Syst.*, vol. 36, no. 2, pp. 549–564, 2000.

[15] E. A. Marranghelli, G. R. López La Valle, and P. A. Roncagliolo, "Orthonormal method for compact Global Navigation Satellite Systems antenna array designs," *Int. J. RF Microw. Comput. Eng.*, vol. 29, no. 12, dec 2019.

[16] A. Papoulis and U. Pillai, *Probability, random variables and stochastic processes*, 4th ed. McGraw-Hill, Nov. 2001.

[17] C. M. Church and I. J. Gupta, "Estimation of adaptive antenna induced code and carrier phase bias in GNSS receivers," *Navig. J. Inst. Navig.*, vol. 56, no. 3, pp. 151–160, jun 2009.

[18] I. J. Gupta, I. M. Weiss, and A. W. Morrison, "Desired Features of Adaptive Antenna Arrays for GNSS Receivers," *Proc. IEEE*, vol. 104, no. 6, pp. 1195–1206, jun 2016.

[19] E. A. Marranghelli, R. L. L. Valle, and P. A. Roncagliolo, "Simple and Effective GNSS Spatial Processing Using a Low-Cost Compact Antenna Array," *IEEE Trans. Aerosp. Electron. Syst.*, vol. 57, no. 5, pp. 3479–3491, may 2021.

[20] H. L. Van Trees, *Optimum Array Processing - Part IV of Detection, Estimation and Modulation Theory*. New York, NY: Wiley, 2002.

[21] T. D. Moore and L. Landau, "Analytic study of STAP and SFAP for RFI suppression (Thesis)," Ph.D. dissertation, 2002.